UNIVERSITY of BRADFORD

Library

The University of Bradford Institutional Repository

http://bradscholars.brad.ac.uk

This work is made available online in accordance with publisher policies. Please refer to the repository record for this item and our Policy Document available from the repository home page for further information.

To see the final version of this work please visit the publisher's website. Access to the published online version may require a subscription.

Link to publisher's version: *https://doi.org/10.1016/j.cej.2018.06.022*

Citation: Al-Obaidi MA, Li J-P, Alsadaie S et al (2018) Modelling and optimisation of a multistage Reverse Osmosis processes with permeate reprocessing and recycling for the removal of N-nitrosodimethylamine from wastewater using Species Conserving Genetic Algorithms. Chemical Engineering Journal. 350: 824-834.

Modelling and Optimisation of a Multistage Reverse Osmosis Processes with Permeate Reprocessing and Recycling for the Removal of N-nitrosodimethylamine from Wastewater using Species Conserving Genetic Algorithms

M. A. Al-Obaidi [1, 2]**, J-P. Li** [1]**, S. Alsadaie** [1]**, C. Kara-Zaïtri** [1] **and I. M. Mujtaba** [1, *]

[1] **School of Engineering, Faculty of Engineering and Informatics. University of Bradford.**
Bradford, West Yorkshire BD7 1DP, UK
[2] **Middle Technical University, Iraq – Baghdad**
*****Corresponding author, Tel.: +44 0 1274 233645**
E-mail address: I.M.Mujtaba@bradford.ac.uk

Abstract

The need for desalinated seawater and reclaimed wastewater is increasing rapidly with the rising demands for drinkable water required for the world with continuously growing population. Reverse Osmosis (RO) processes are now among the most promising technologies used to remove chemicals from industrial effluents. N-nitrosamine compounds and especially N-nitrosodimethylamine (NDMA) are human carcinogens and can be found in industrial effluents of many industries. Particularly, NDMA is one of the by-products of disinfection process of secondary-treated wastewater effluent with chloramines, chlorines, and ozone (inhibitors). However, multi-stage RO processes with permeate reprocessing and recycling has not yet been considered for the removal of N-nitrosodimethylamine from wastewater. This research therefore, begins by investigating a number of multi-stage RO processes with permeate-reprocessing to remove N-nitrosodimethylamine (NDMA) from wastewater and finds the best configuration in terms of rejection, recovery and energy consumption via optimisation. For the first time we have applied Species Conserving Genetic Algorithm (SCGA) in optimising RO process conditions for wastewater treatment. Finally, permeate recycling is added to the best configuration and its performance is evaluated as a function of the amount of permeate being recycled via simulation. For this purpose, a mathematical model is developed based on the solution diffusion model,

which is used for both optimisation and simulation. A number of model parameters have been estimated using experimental data of Fujioka et al. [13] (Journal of Membrane Science 454 (2014) 212–219), so that the model can be used for simulation and optimisation with high accuracy and confidence.

Keywords: Multi-stage Reverse Osmosis Processes; Permeate Reprocessing; Permeate Recycle; Species Conserving Genetic Algorithm Optimisation (SCGA); N-nitrosamine Removal.

1. Introduction

The reuse of recycled water continues to offer a practical and promising solution for resolving water shortage problems in several arid regions and developing countries. Water reuse reduces the challenges of increasing freshwater supply cost as well as mitigates environmental pollution. This readily explains the significant increase of upgraded wastewater and water reclamation plants across the world and especially in Europe [1,2]. However, the existence of pollutants such as N-nitrosamine in drinking and reused water resources continues to pose a real threat to public health and safety. N-nitrosamines compounds and especially N-nitrosodimethylamine (NDMA) (hydrophilic compound) are human carcinogens that can be formed in a range of industrial processes and discharged into secondary effluents. Particularly, chloramines, chlorines, and ozone (potential oxidants) can react with amines in the disinfection process of secondary-treated wastewater effluent to form NDMA [3]. They therefore pose a high risk to drinking water for humans and animals due to their highly toxicological effects [4,5]. Accordingly, many water authorities are now regulated against a strict allowable N-nitrosamine concentration level in drinking water and recycled water. For instance, the US Environmental Protection Agency (US

EPA) has strictly limited N-nitrosamine at 0.7 ng/L (which is equivalent to 0.7×10^{-9} kg/m³) to discharge due to the possibility of cancer risk to human at this concentration [6]. However, the notification level of NDMA was set at 10 ng/L and 1 ng/L in drinking water by the California Department of Public Health and the Ministry of Environment of Ontario respectively [7,8]. Generally, the use of UV/H_2O_2 irradiation process has proved to be efficient for destroying NDMA. Other treatments, such as activated carbon adsorption, ozonation and sand filtration have not been so successful [9]. However, the UV/H_2O_2 technology not only consumes a lot of energy, but it also potentially increases the risk of increasing the carbon concentration of the reused water [10]. In this respect, the use of RO process is progressively increased as a projecting approach in response to avoid the need for costly conventional methods and to satisfy the requirements of very low limits of high toxic compounds. The performance of RO process is mainly dependent on several parameters including the operating conditions (feed concentration, pressure, flow rate and temperature) and the design (RO configuration). Having said this, the Reverse Osmosis (RO) process has been extensively used to abate organic compounds from wastewater, with an efficiency for eliminating NDMA from wastewater in the range $40 - 70\%$. There are several reasons for this, one being the uncharged properties of NDMA as well as it small molecular size which facilitates high permeation through the membrane [11,12].

Fujioka et al. [13] used a full-scale retentate reprocessing design of three spiral wound RO membranes connected in a series configuration and confirmed a range of 40 to 61% NDMA removal. More recently, Fujioka et al. [14] have improved the NDMA removal to 92% based on an immersion of RO membranes in high-temperature ultrapure water. One possible explanation of this is the fact that heat treatment may tighten the membrane structure and therefore improve the removal of NDMA. However, the main drawback of this treatment was a substantial

reduction of water recovery. It is evident in their work that heat treatment has reduced the water permeability constant of the membranes in the range of 20 to 35% of several types of membranes compared to untreated membranes. This means that the stubborn NDMA existence in wastewater remains a challenge, which has motivated the authors to find a suitable solution but without heat treatment.

A starting point of the research is to examine the permeate reprocessing and recycling technique. This is in fact a compulsory choice due to the stringent limits of permeate concentration of some impurities. Interestingly, Magara et al. [15], Redondo et al. [16], and Farhat et al. [17] alleviated the boron concentration in drinking water with promising results after using the permeate reprocessing design.

The open literature contains several studies using Genetic Algorithms (GA) to optimise the performance of seawater and wastewater treatment processes [18 – 25]. Recently, Al-Obaidi et al. [26] used GAs to maximise the rejection of chlorophenol from wastewater. Holland [27] confirmed that the GA optimisation technique can yield better results compared to other conventional methods. However, engineering optimisation problems are very complex as they are multimodal in nature. In order to let GAs cope with multimodal problems and not be constrained in a local solution, several techniques have been developed. They include crowding [28], fitness share [29] and species conserving GA [30]. Species conserving GA (SCGA) can generally find multiple solutions of the optimisation problem at the end of each iteration, as opposed to a single solution. This approach provides a wide opportunity to select the proper optimized solution for any input data of operation. In other words, the SCGA will aid the optimiser to select the best optimal solution from a bunch of optimal solutions which would satisfy certain process requirements. In this paper, a Species Conserving Genetic Algorithm

(SCGA) of Li et al. [30] will be applied to the proposed RO process for the removal of NDMA from wastewater.

1.1 Novelty and contribution of this work

To the best of authors' knowledge, there has not yet been any study utilising the permeate reprocessing design for removing NDMA using multi-stage RO process. Here, a multi-stage RO system is proposed with the retentate and permeate reprocessing option. As we aimed to explore and assess the performance of a number of configurations of multi-stage RO process with different permeate reprocessing scheme in this work, it is not economically feasible to achieve it via laboratory experiments. Hence, a high fidelity model validated against reliable experimental data of Fujioka et al. [13] is used. Note, Fujioka et al. [13] carried out the experiments using seven elements of spiral wound membranes each with an area of 7.9 m^2 in series configuration. However, in this work, we used a total of 18 membrane elements each having 37.2 m^2 area of the same geometry used by Fujioka et al. [13] to create several configurations. Therefore, the model developed in this work based on the experimental data is valid for our multi-stage configurations. In the past, Genetic Algorithm has been used for optimising RO process for wastewater treatment. However, in this work, for the first time we have used Species Conserving Genetic Algorithm (SCGA) to optimise process conditions. Three important indicators of performance (a) high NDMA rejection (b) recovery rate and (c) energy consumption are used to select the best RO configuration. Finally, a permeate recycling option is added to the best configuration and further simulation is carried out to investigate the effect of recycling on rejection, recovery, and energy consumption.

2. Previous experimental work of Fujioka et al. [13]

Fujioka et al. [13] used a full-scale cross-flow RO filtration system of seven 4″ glass-fiber pressure vessels in series (each pressure vessel holds one spiral-wound membrane element) to remove NDMA from N-nitrosamine stock solution containing 10 mg/L of several N-nitrosamine solutes including NDMA (Fig. 1). The N-nitrosamine solution was prepared in pure methanol besides aqueous feed stock solutions of NaCl, $CaCl_2$ and $NaHCO_3$ were prepared in Milli-Q water at 2M (NaCl) and 0.1 M ($CaCl_2$ and $NaHCO_3$) concentrations to imitate the electrolyte composition found in the secondary or tertiary treated wastewater. Then, the two stock solutions are mixed to obtain approximately 250 ng/L (3.3761×10^{-9} kmol/m³) of NDMA.

The RO experiments started by filling the feed tank with the model wastewater considering full batch system where both the concentrate and permeate streams are recycled back into feed tank to keep fixed feed concentration. In this respect, the feed was pumped at fixed feed flow rate of 2.43×10^{-3} m³/s, while the operating feed pressure has been increased from 4, 6.5 and 10.1 atm to adjust average permeate flux at 2.78×10^{-6}, 5.56×10^{-6} and 8.33×10^{-6} m/s respectively during the experiments. However, the operating temperature was kept at 20±0.1 °C along the experiments.
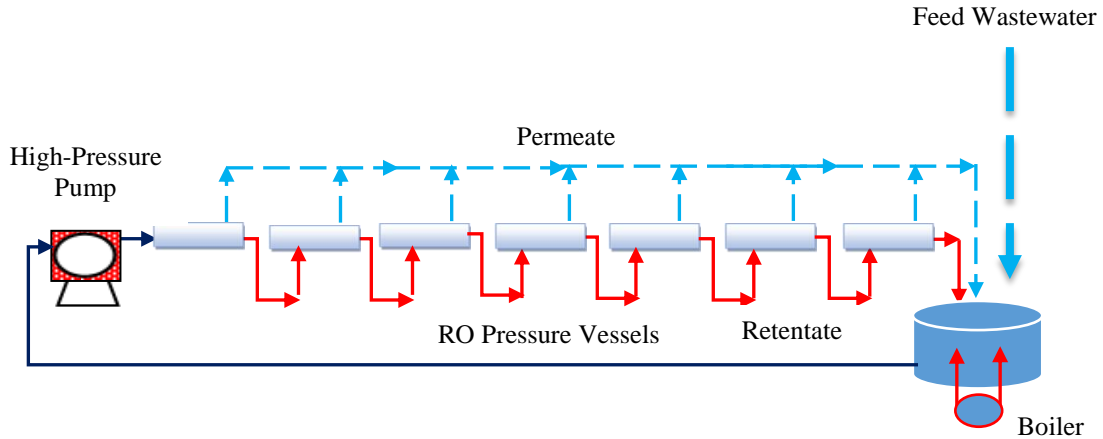
Fig. 1. Schematic diagram of full-scale seven elements RO plant (Fujioka et al. [13])

2. Modelling of the spiral wound RO process

The mathematical modelling of the membrane module facilitates simulation and optimisation studies required for identifying the most effective design of the system [31]. The main objective of this section is to establish a mathematical model to predict accurately the performance of a spiral wound RO process for the rejection of N-nitrosamine compounds from aqueous solutions. For this to happen, the transport phenomena of water and solute through the membrane need to be represented mathematically for building an appropriate process model, which will incorporate the calculations of the fluid properties.

Al-Obaidi et al. [32,33] have developed two distributed mathematical models based on the solution diffusion model and irreversible thermodynamic model to predict the performance of single and multi-stage spiral wound RO process for the removal of N-nitrosamine from wastewater. However, these models have not considered the feed spacer characteristics and the

7

impact of operating temperature on the transport parameters. In this paper, a new mathematical steady state model is developed for the removal of NDMA from wastewater.

2.1 Assumptions

The following assumptions are applied to develop the proposed model:

1. The solution diffusion model is used for mass transport through the module.

2. The membrane characteristics and the channel geometries are assumed constant.

3. Validity of the Da Costa equation to predict the pressure drop across the membrane.

4. Validity of the film model theory to estimate the concentration polarisation impact.

5. Constant atmospheric pressure at the permeate channel of 1 atm.

6. The underlying process is assumed to be isothermal.

7. Constant pump and energy recovery device efficiencies of 80 and 90% respectively.

2.2 Governing equations

Based on Assumption 1, the solution diffusion model can be used to predict the water and solute flux J_w and J_s (m/s, kg/m² s) through the membrane as expressed by Lonsdale et al. [34].

$$J_w = A_w \left[\left(\frac{(P_{f(in)} + P_{f(out)})}{2} - P_p \right) - (\Delta \pi_{Total}) \right] \tag{1}$$

$$J_s = B_s \left(C_m - C_p \right) \tag{2}$$

Where A_w and B_s (m/atm s, m/s) are solvent and NDMA transport coefficients respectively. $P_{f(in)}$, $P_{f(out)}$ and P_p (atm) are inlet feed pressure, retentate pressure and permeate pressure respectively.

The total osmotic pressure difference of NDMA $\Delta \pi_{Total}$ can be described in Eq. (3).

$$\Delta \pi_{Total} = \left(\pi_m - \pi_p \right) \tag{3}$$

Where π_m (atm) is the osmotic pressure of NDMA at the membrane wall concentration C_m (kg/m³), while π_p (atm) is the osmotic pressure at permeate channel regarding the permeate concentration C_p (kg/m³). The estimation of the feed and permeate osmotic pressure can be obtained using Eqs. (4) and (5) [13].

$$\pi_m = 1.19 \, (T + 273.15) \left(\frac{C_m}{Mwt} \right) \tag{4}$$

$$\pi_p = 1.19 \, (T + 273.15) \left(\frac{C_p}{Mwt} \right) \tag{5}$$

Mwt, T (kg/kmol, °C) are the molecular weight of NDMA provided in Table 3 and operating temperature respectively. The concentration of NDMA at the wall membrane was estimated based on Assumption 4, which in turn is based on the validity of the film model theory where the solvent flux is linked to concentration polarization and mass transfer coefficient k, using the following equation:

$$\frac{(C_m - C_p)}{(C_b - C_p)} = exp \left(\frac{J_w}{k} \right) \tag{6}$$

C_b, k (kg/m³, m/s) are the bulk concentration in the feed channel and the mass transfer coefficient for NDMA respectively. C_b is taken the average value of feed C_f and retentate C_r concentrations using Eq. (7).

$$C_b = \frac{C_f + C_r}{2} \tag{7}$$

The mass transfer coefficient k (m/s) for NDMA is a function of pressure, concentration, flow rate, and temperature, which is calculated using the proposed equation of Winograd et al. [35]. This is an empirical equation which takes into account the impact of geometry of feed spacer and feed flow channel, dynamic viscosity and solute diffusivity.

$$k = 0.753 \left(\frac{K}{2-K} \right)^{0.5} \left(\frac{D_b}{t_f} \right) \left(\frac{\mu_b \, \rho_b}{D_b} \right)^{0.1666} \left(\frac{2 \, t_f^2 \, U_b}{D_b \, \Delta L} \right)^{0.5} \tag{8}$$

$K, D_b, \mu_b, \rho_b, t_f, \Delta L$ and U_b are the efficiency of mixing net (i.e. spacer) (K = 0.5) (dimensionless) [13, 36], diffusion coefficient (m²/s), dynamic viscosity (kg/m s), density (kg/m³), feed channel height (m), characteristic length of mixing net (m) and feed velocity (m/s) respectively. The estimation of diffusion coefficient D_b and density ρ_b is carried out using the water equation of Koroneos [37] due to the very dilute aqueous solutions of NDMA, which were considered in this study as follows:

$$D_b = 6.725x10^{-6} \ exp \left\{ 0.1546x10^{-3} \ C_b - \frac{2513}{T+273.15} \right\} \tag{9}$$

$$\rho_b = 498.4 \ m_f + \sqrt{\left[248400 \ m_f^2 + 752.4 \ m_f \ C_b \right]} \tag{10}$$

$$m_f = 1.0069 - 2.757x10^{-4} \ T \tag{11}$$

The viscosity coefficient μ_b (kg/m s) is calculated using Eq. (12) [13].

$$\mu_b = 2.141x10^{-5} \ x \ 10^{\left(\frac{247.8}{(T+273.15)-140)} \right)} \tag{12}$$

The bulk feed velocity U_b (m/s) is calculated using Eq. (13).

$$U_b = \frac{Q_b}{W \ t_f \ \epsilon} \tag{13}$$

Q_b, W and ϵ (m³/s, m, dimensionless) are the bulk feed flow rate, which is calculated using Eq. (14), membrane width and void fraction of the spacer respectively.

$$Q_b = \frac{Q_f + Q_r}{2} \tag{14}$$

Q_f and Q_r (m³/s) are the feed and retentate flow rates.

The process of NDMA rejection is accompanied by a pressure drop along the membrane edges. Therefore, the retentate pressure $P_{f(out)}$ (atm) is calculated using Eq. (15).

$$P_{f(out)} = P_{f(in)} - \Delta P_{drop} \tag{15}$$

ΔP_{drop} (atm) is the pressure drop of the spiral wound element, which is calculated using the proposed correlation of Da Costa et al. [38] (Eq. 16) in line with Assumption 3. Da Costa et al. [38] assumes that the pressure and kinetic losses occur due to drag on the feed spacer and a change in direction of flow respectively. In fact, they neglect the friction losses at the channel walls and on the spacer surface.

$$\Delta P_{drop} = \left(\frac{\rho_b \ U_b^2 \ L \ C_{td}}{2 \ d_h}\right) x \ 9.8692 x 10^{-6} \tag{16}$$

C_{td}, d_h (dimensionless, m) are the total drag coefficient, which is calculated using Eq. (17) and hydraulic diameter of the feed spacer channel respectively. L (m) is the membrane length.

$$C_{td} = \frac{A'}{Re^n} \tag{17}$$

A' and n (dimensionless) are the spacer characteristics. Also, the Reynolds number Re (dimensionless) is calculated using Eq. (18).

$$Re = \frac{\rho_b \ d_h \ U_b}{\mu_b} \tag{18}$$

d_h (m) is the hydraulic diameter, while the overall solute and mass balance equations of the unit are given by Eqs. (19) and (20).

$$Q_f = Q_r + Q_p \tag{19}$$

$$Q_f \ C_f = Q_r \ C_r + Q_p \ C_p \tag{20}$$

C_f, C_r and C_p (kg/m³) are the concentration of NDMA in feed, retentate and permeate channel respectively. Also, Eq. (21) is used to calculate the concentration at the permeate channel for NDMA [26].

$$C_p = \frac{C_f \ B_s}{B_s + \frac{J_w}{\exp(\frac{J_w}{k})}} \tag{21}$$

The rejection parameter Rej (dimensionless) of NDMA can be calculated using Eq. (22).

$$Rej = \frac{C_f - C_p}{C_f} \, x100 \tag{22}$$

The total recovery Rec (dimensionless) of a single module can be calculated using Eq. (23).

$$Rec = \frac{Q_p}{Q_f} \, x100 \tag{23}$$

Q_p (m³/s) is the total permeated flow rate, which can be calculated using Eq. (24).

$$Q_p = J_w \, A$$

A (m²) is the effective membrane area.

The total energy consumption $EC1$ (kWh/m³) of any stage of RO system measured in kWh per m³ of the total permeate is calculated using Eq. (24) of Qi et al. [39] based on the use of a high-pressure pump.

$$EC1 = \frac{\frac{\left(\left(P_{f(in)} \, x101325\right) Q_f\right)}{Q_p \, \varepsilon_{pump}}}{36x10^5} \tag{24}$$

In case of using an energy recovery device ERD in the RO process network, the calculation of the total energy consumption $EC2$ (kWh/m³) is carried out using Eq. (25). More specifically, the energy performance of the conventional pilot-plant is calculated in respect of the outgoing and ingoing entering energies.

$$EC2 = \frac{\frac{\left(P_{f(in)} \, x101325\right) Q_f}{Q_p \, \varepsilon_{pump}} - \frac{\left(P_{f(out)} \, x101325\right) Q_r \, \varepsilon_{ERD}}{Q_p}}{36x10^5} \tag{25}$$

Eq. (26) can be used to calculate the outlet pressure of ERD $P_{f(out)(ERD)}$, which will be used in next stage for the outlet pressure of membrane modules of the previous stage $P_{f(in)(ERD)}$.

$$\varepsilon_{ERD} = \frac{P_{f(out)(ERD)}}{P_{f(in)(ERD)}} \tag{26}$$

Finally, the feed temperature T has an impact on the physical properties and the transport membrane constants, A_w and B_s. Therefore, Eqs. (27) and (28) are investigated the impact of temperature on these parameters as follows [40]:

$$A_{w(T)} = A_{w(T_o)} \frac{\mu_{b(T_o)}}{\mu_{b(T)}} \tag{27}$$

$$B_{s(T)} = B_{s(T_o)} \frac{(T+273.15)}{(T_o+273.15)} \frac{\mu_{b(T_o)}}{\mu_{b(T)}} \tag{28}$$

$A_{w(T_o)}$ and $B_{s(T_o)}$ are the permeate and NDMA transport parameters at reference temperature. The process model of nonlinear algebraic equations shown in Section 2.2 is written in the compact form of: $g(z,\ u,\ v) = 0$.

- z is the set of all algebraic variables,

- u is the set of decision variables need to be optimised and

- v represents the constant parameters of the model.

- The function g is assumed to be continuously differentiable with respect to all their arguments.

The model developed was implemented on the gPROMS software suite [41].

2.3 Determination of transport parameters

One of the main requirements of testing the proposed model in simulation mode is that the unknown parameters of the model should be estimated based on reliable experimental data. These parameters include; the water permeability constant A_w, the NDMA transport parameter B_s and the spacer characteristics of A' and n. In this research, the experimental data of Fujioka et al. [13] who considered a set of seven elements of spiral wound membranes arranged in series configuration with initial conditions of 6.51 atm, 2.43x10^{-3} m³/s, 2.5x10^{-7} kg/m³ (250 ng/L) and

20 ℃ are used to predict the best values of the unknown parameters of the proposed model. The parameters are estimated using the gEST tool of the gPROMS software suite. The estimated dimensions of the spacer mesh (A' and n) were found to be close to the spacer type CONWED-1 as reported in the study of Da Costa et al. [38] ($A' = 1.29$ and $n = 0.24$). The results of parameter estimation are given in Table 1.

Table 1. Parameter estimation results at 20 °C

Parameter	A_w (m/s atm)	B_s (m/s)	A' (dimensionless)	n (dimensionless)
value	6.904×10^{-7}	5.59×10^{-6}	1.21	0.27

2.4 Reliability of the model and model validation

In this work, we have used exactly the same geometry membrane module as used by Fujioka et al. [13] so that the model developed based on the experimental data can be used reliably for further model-based studies (as is the focus of this work).

Table 2 provides a comparison of experimental and predicted values of retentate plant pressure $P_{f(out)}$, total permeate flux J_w and total NDMA rejection Rej showing a very good match of marginal absolute errors. The validated model can therefore be used to carry out an optimisation study of several selected multi-stage RO process of permeate-reprocessing and recycling as described below.

14

Table 2. Model validation results

$P_{f(out)}$ (atm)		Absolute Error %	J_w (m/s) x10^6		Absolute Error %	C_p (kg/m³) x10^9		Absolute Error %	Rej (-)		Absolute Error %
Exp.	The.		Exp.	The.		Exp.	The.		Exp.	The.	
4.697	4.697	0.0	3.158	3.178	0.64	2.39	2.191	8.31	35.08	35.09	0.02

3. Description of permeate reprocessing multi-stage RO process

Although multi-stage RO permeate reprocessing option has been considered in seawater desalination, this option has not been considered in wastewater treatment in the past specially for NDMA removal from wastewater. In this work, for the first time, several configurations with multi-stage RO permeate reprocessing option are proposed and optimised in terms of NDMA removal from wastewater and energy consumption.

To increase the NDMA rejection from wastewater as found in the literature, Fig. 2 shows schematic diagrams of five configurations (A to E) of permeate recycling of multi-stage RO process, which will be used to investigate. The configurations are based on the mixing of the collected permeate of stage 1, feed it to stage 2, and so on. Moreover, the use of energy recovery device (ERD) is inevitable for transferring the potential energy from the high-pressure streams to the low-pressure streams of each stage, which in turn reduces the issue of high energy consumption for the proposed design. In the end, the collected low-pressure retentate streams of all the stages are disposed of. Each configuration contains six pressure vessels connected in different arrangements of stages. Three elements of spiral wound RO membrane type BW30-400 of 37.2 m² (effective membrane area) produced by Dow/FilmTec and connected in series were inserted inside each pressure vessel. The technical details of the membrane used, spacer characteristics, friction factor and the water and NDMA transport parameters are given in Table

3. The selection of the configurations of Fig. 2 is based on the allowed manufacturer operating limits of feed flow rate of each stage and element. Pump (maximum of 40.46 atm) and energy recovery efficiencies are assumed to be 80 and 90% respectively.
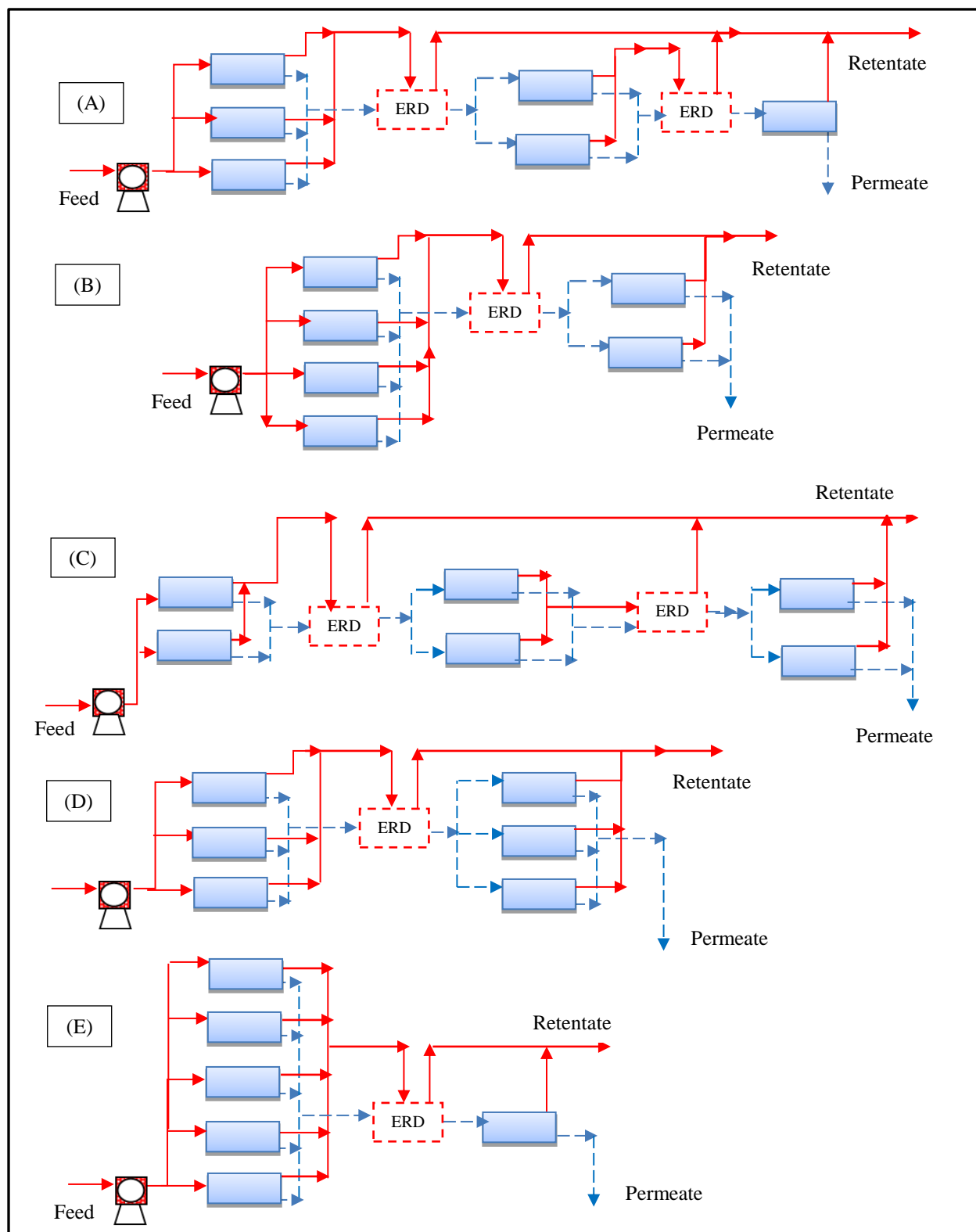
Fig. 2. Schematics of various configurations of multi-stage permeate reprocessing RO system

17

Table 3. Specifications of the spiral wound membrane element [42]

Make	Dow/FilmTec
Membrane type and configuration	BW30-400, Spiral-wound, Polyamide Thin-Film Composite
Feed and permeate spacer thickness t_f (m)	5.93×10^{-4}
Hydraulic diameter of the feed spacer channel d_h (m)	8.126×10^{-4}
Effective membrane area A (m²)	37.2
Membrane length L and width W (m)	1 and 37.2
A_w (m/ atm s) at reference temperature of 28.8 °C	9.5096×10^{-7}
B_s (NDMA) (m/s) at reference temperature 20 °C *	5.35×10^{-6} *
Mwt_{NDMA} (kg/kmol) *	74.05
Spacer type	(NALTEX-151-129)
A' (dimensionless)	7.38
n (dimensionless)	0.34
ε (dimensionless)	0.9058

*: Fujioka et al. [13]

4. Optimisation of permeate reprocessing RO system

4.1 Problem description and formulation

This section deals with the optimisation of the proposed configurations A to E shown in Fig. 2 using the SCGA technique. The inlet feed concentration of NDMA for all configurations is 1×10^{-6} kg/m³ (1000 ng/L) which is same as that of Fujioka et al. [14]. The final NDMA rejection ($Rej_{(NDMA)}$) and energy consumption (EC) are chosen as the two objective functions for the optimisation problem where NDMA rejection is maximised and EC is minimised simultaneously for each configuration (A to E), while optimising the operating conditions of plant feed pressure,

flow rate and temperature. The lower and upper bounds of the feed flow rate for each membrane, operating pressure and temperature are set as constraints of the optimisation problem. We considered a maximum pressure drop of 0.987 atm for each membrane element as given in Table 4.

The mathematical description of the optimisation problem of the RO process with permeate reprocessing design is illustrated below:

$$Max \qquad\qquad\qquad Rej_{(NDMA)}(-)$$

$$Min \qquad\qquad\qquad EC\ (kWh/m^3)$$

$$Q_{f(plant)}, P_{f(plant)}, T_{(plant)}$$

Subject to:

      Equality constraints:

          Process Model $\qquad\qquad g(z,\ u,\ v) = 0$

Inequality constraints of the plant:

$$Q_{f(plant)}{}^{L} \leq Q_{f(plant)} \leq Q_{f(plant)}{}^{U}$$

$$(10\ atm)\ P_{f(plant)}{}^{L} \leq P_{f(plant)} \leq P_{f(plant)}{}^{U}\ (40.463\ atm)$$

$$(20\ ^{\circ}C)\ T_{(plant)}{}^{L} \leq T_{(plant)} \leq T_{(plant)}{}^{U}\ (45\ ^{\circ}C)$$

Inequality constraints of the element:

$$(1.008 \times 10^{-3}\ m^3/s)\ Q_{f}{}^{L} \leq Q_{f} \leq Q_{f}{}^{U}\ (5.363 \times 10^{-3}\ m^3/s)$$

$$(10\ atm)\ P_{f(in)}{}^{L} \leq P_{f(in)} \leq P_{f(in)}{}^{U}\ (40.463\ atm)$$

$$(20\ ^{\circ}C)\ T^{L} \leq T \leq T^{U}\ (45\ ^{\circ}C)$$

$$\Delta P_{drop} \leq 0.987\ (atm)$$

It is important to note that the maximum and minimum limits of the plant feed flow rates $Q_{f(plant)}$ depend on the number of parallel pressure vessels in the first stage.

Table 4. The limits of operation of the spiral-wound membrane element [42]

Parameter	Value
Max. operating temperature T (°C)	45
Max. operating pressure (atm)	40.463
Max. pressure drop (atm)	0.987
Max. feed flow rate (m³/s)	5.363×10^{-3}
Min. feed flow rate (m³/s)	1.008×10^{-3}

4.2 The characteristics of Species Conserving Genetic Algorithm (SCGA)

Although Genetic Algorithm (GA) based optimisation technique has been used for several industrial applications such as thermal cracking [43] and RO wastewater treatment [26], for the first time, we applied Species Conserving Genetic Algorithm (SCGA) based optimisation technique in RO wastewater treatment process. SCGA [30] has already been demonstrated [44] as an effective method for searching for several solutions for complex optimisation problems. This will be used for selecting appropriate operating conditions. Interestingly, the SCGA generates multiple solutions for each optimisation problem, which provides the option of selecting the most appropriate solution.

A species is the fundamental concept of the SCGA and described as a set of individuals with similar characteristics. In a population, a species s_i is around its species seed x^* (the best individual), if for everyone $y \in s_i$

$$d(x^*, y) < r_s \tag{29}$$

20

and

$$f(y) \leq f(x^*) \tag{30}$$

Where $d(*,*)$ is to calculate the distance between two individuals and r_s is the species radius.

Fig. 3 **Error! Reference source not found.**shows the species distribution in a 2D space. A species consists of some individuals and takes a portion of the feasibility region. Some individuals are located in the intersection of several spaces. The pseudocodes of the SCGA [30] is illustrated in Fig. 4, where $G(t)$ denotes the population at time t and X_s denotes the species set.
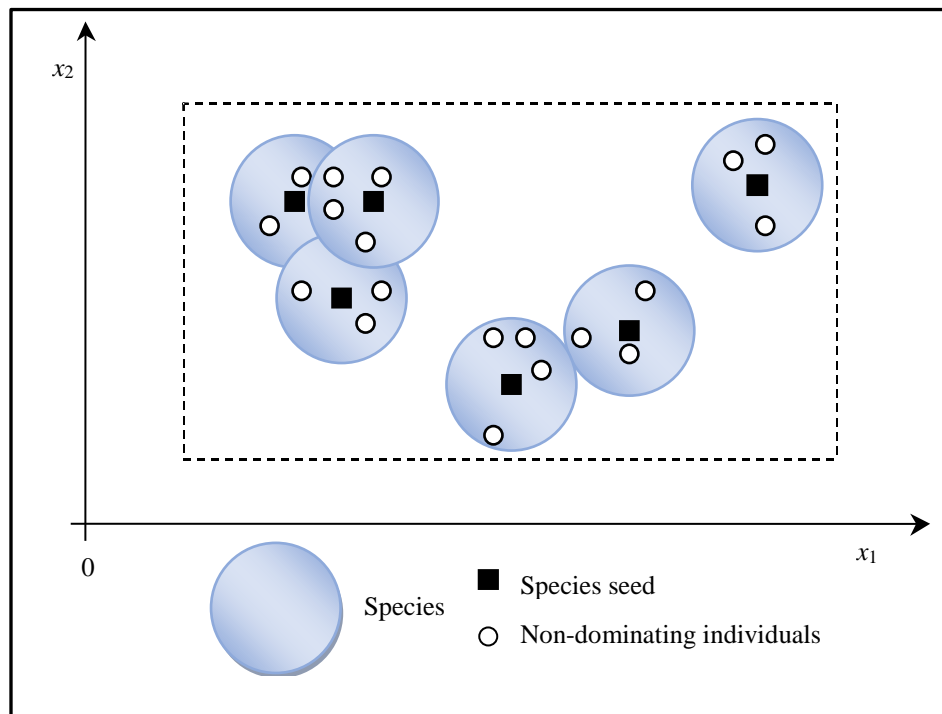

Fig 3. A distribution of species in a 2D space.

```
Begin
    t = 0;
    Initialize G(t);
    Evaluate G(t);
    while (not termination condition) do
        Determine species seeds X_s;
        Select G(t+1);
        Crossover G(t+1);
        Mutate G(t+1);
        Evaluate G(t+1);
        Conserve species from X_s in G(t+1);
        t = t+1;
    end (while)
    Identify global optima;
End
```

Fig. 4. The pseudocodes of the SCGA

The population is dynamically separated in a SCGA into several groups, called species, based on the similarities and each is built around its species seed. The principle of the SCGA is to find species and keep them in order to survive in the future generations.

Compared with a traditional genetic algorithm, there are three special operators in the SCGA:

1. Identifying species seeds: The operator is designed to search species from a current population. At the beginning, all the individuals are marked as unprocessed. A best unprocessed one is picked up to be a species seed and all members which distance to the species seed is less than the species radius are recorded as "processed". This procedure

will be repeated until all the individuals have been processed. All the species seed will be saved in the set, X_s.

2. Conserving species seeds: After the population is built by using the genetic operations, the species will be conserved and copied from the species set, X_s back to the new population.

3. Determining global solutions: As the best individual in a species seeds is saved in the set x_s, the simple way to identify solutions is to select the best species from x_s. A *threshold* r_f $(0 < r_f \leq 1)$ is applied for this purpose. A species seed x in the species set (X_s) is treated as a solution, if:

$$f(x) \leq f_{max} - (f_{max} - f_{min}) \, r_f \tag{31}$$

Where f_{min} and f_{max} are the best and worst objective value.

The default value of species radius is set as 1 in this paper.

Basically, SCGA can only solve problems with a single objective. The above problem in Section 4.1 has two objectives and therefore a in new single objective is developed as given in Eq. (32) to be compatible with SCGA requirements

$$f\left(Q_{f(plant)}, P_{f(plant)}, T_{(plant)}\right) = W_1 \times Rej_{(NDMA)} + W_2 \times \left(\frac{1}{EC}\right)$$

(32)

W_1 and W_2 are the weighting factors. Therefore, the original problem is changed to maximise the objective function in Eq. (32). In this paper, two objectives are the same important. The maximum value of $Rej_{(NDMA)}$ is set as 1 to simplify the analysis and the maximum value of EC is about 5. Then, let W_1 to be 1, then W_2 should be 5, which means both objectives are the same important level and have the same contribution of the system objective.

4.3. The optimisation results

The multi-objective optimisation problem is solved by using the SCGA platform linked with the model of Section 2.2 considering the multi-stage RO process with permeate reprocessing configuration (Fig. 2). To fulfil the requirements of the optimisation platform using SCGA the process model presented in Section 2 has been written in C++. Table 5 shows the optimisation results of the configurations A to E with plant feed concentration $C_{f(plant)}$ of 1000 ng/L (1×10^{-6} kg/m³) with the optimised plant feed pressure, flow rate and temperature. Due to its inherent property, the SCGA method has provided several optimum solutions for each selected configuration A to E. The nondominated solution is shown in bold in Table 5.

Table 5. Optimisation results of configurations A to E (fresh feed concentration: $C_{f(plant)}$=1000 ng/L),

| Configuration | Solutions | The decision variables | | | $Rej_{(NDMA)}$ | $Rec_{(plant)}$ | $C_{p(plant)} \times 10^8$ | EC |
		$Q_{f(plant)}$ (m³/h)	$P_{f(plant)}$ (atm)	$T_{(plant)}$ (°C)	(-)	(-)	(kg/m³)	(kWh/m³)
A	1	30.348	27.5	20	92.17	20.98	7.38	3.37
	2	43.2	32.2	22.3	94.6	17.2	5.40	4.78
	3	46.692	30.2	27.4	94.22	17.5	5.78	4.42
	4	42.66	27.39	29.71	93.25	18.18	6.75	3.85
B	1	59.616	31.28	20.0	87.01	27.32	13.00	2.96
	2	76.608	26.95	20.65	87.47	18.16	12.50	3.12
C	**1**	**38.592**	**38.45**	**22.68**	**90.21**	**50.15**	**9.79**	**1.96**
	2	38.628	35.96	20.60	90.17	44.39	9.83	1.96
D	1	57.924	36.24	20	82.24	49.55	17.80	1.78
	2	57.384	40.17	20.06	82.0	55.93	18.00	1.87
	3	49.5	34.19	20.02	80.25	54.97	19.80	1.60
E	1	59.328	13.64	20.0	79.07	5.34	20.90	4.77

	2	50.58	13.22	20.54	77.93	6.20	22.10	4.22

A close look at the results shows that the permeate reprocessing design has significantly improved the removal of NDMA compared with the findings of the literature, which approximately ranged between 40 – 70% [9,11,12] except that of Fujioka et al. [14] (92% rejection was obtained but under heat treatment with a substantial reduction of water transport parameter and recovery rate). Interestingly, solution A1 is close to that obtained by Fujioka et al. [14] in terms of rejection. Cleary, all cases show that rejection increases with lower recovery rate. However, only configurations C and D have achieved high recovery rate compared to other configurations tested. Interestingly, the recovery of configurations E and A is the worst one. The presence of only one pressure vessel in the last stage can explain the main reason for this. Note that configuration E has the lowest recovery due to the higher feed flow rate of augmented permeate streams of five pressure vessels that fed to the final module compared to only two pressure vessels in configuration A. This in turn increases the bulk velocity inside the last module leading to a lower recovery rate. In the same respect, the recovery rate of configuration E is not comparable with configuration B (Table 5). To explain this concern, both configuration B and E are simulated at same operating conditions of 1000 ng/L, 59.328 m³/h, 13.64 atm, and 20 °C of feed concentration, flow rate, pressure, and temperature respectively. It is evident that the first stage of configuration B has generated 25.7% of recovery lower than the first stage of configuration E (32.5%). However, the second stage of configuration B has generated 42.8% of recovery rate compared to only 16.4% of configuration E. Finally, the total plant recovery rate of configuration B is 11% compared to 5.3% of configuration E. Therefore, it can be said that reduction in the bulk velocity can increase the permeate recovery. In terms of rejection, solution

A2 is the best where the NDMA concentration is reduced from $1x10^{-6}$ kg/m³ to $5.4x10^{-8}$ kg/m³ (which is equivalent to 54 ng/L). Note that the allowed NDMA concentration is 0.7 ng/L according to US EPA [6]. However, solution E2 is the worst in terms of solute rejection. In terms of recovery, solution D2 is the best and E2 is the worst. In terms of energy consumption, solution A2 is the worst, solution D3 is the best. Clearly, performance of E is the worst compared to all cases. However, looking at all 3 parameters (rejection, recovery, energy consumption) simultaneously, solution C1 stands out as the best (subjective decision). In terms of rejection, it is about 4% down compared to A2. In terms of recovery, C1 is 10% down compared to D2. In terms of energy consumption C1 is up by about 18% up compared to D3 but 60% down compared to A2. For completeness, the final concentration of NDMA in the permeate is presented in Table 5 for all cases.

5. The permeate reprocessing and recycling of multi-stage RO process

Section 4 dealt with permeate reprocessing only. In this section we consider permeate reprocessing combined with the permeate recycling option. Instead of applying recycling in all the configurations considered in Section 4, we only applied it on the best configuration identified in Section 4; i.e. configuration C. Fig. 5 shows a schematic diagram of the proposed multi-stage permeate reprocessing-recycling RO process (Configuration F). The main characteristics of this process is that a portion of permeate is recycled back to the feed stream at a constant plant feed flow rate. Thus, the feed flow rate of stage 1 will be increased as the recycled stream increases. Accordingly, the model developed of Section 2.2 has been calibrated to include the requirements of this configuration.
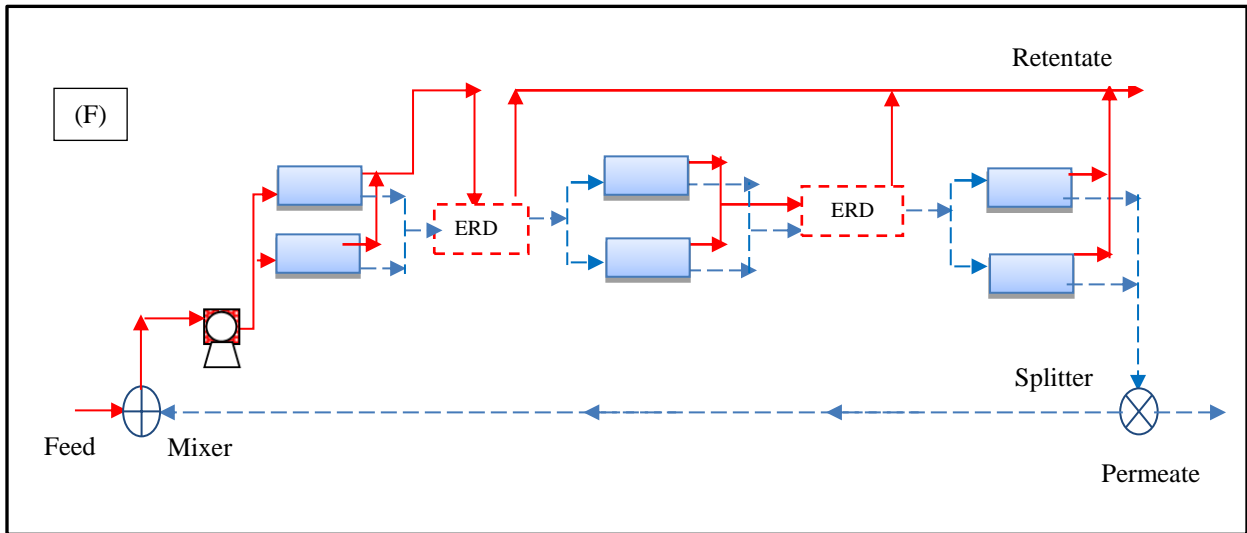
26

Fig. 5. Tested configuration of multi-stage permeate reprocessing-recycling RO design

5.1. Results of the permeate reprocessing-recycling of multi-stage RO process

Fig. 6 shows the impact of permeate recycling from the last stage of Configuration F (Fig. 5) on the total permeate concentration of NDMA and plant recovery rate. Note, zero permeate recycle corresponds to the results of Configuration C1 (Solution 1 in Table 5). The results show that increasing permeate recycle decreases both the permeate concentration and the recovery rate. The higher the permeate recycle to the inlet feed stream, the higher the reduction in the inlet feed concentration of the first stage. This will reduce the concentration polarisation and in turn will increase the mass transfer coefficient and will reduce the solute flux through the membrane. However, this will also cause an increase in the inlet feed flow rate throughout all stages. Therefore, it is expected that the feed velocity of all the stages will increase and this in turn will cause a higher pressure-drop along each module. As a result, this would diminish the passage of water through the membrane and finally reduces the recovery rate (Fig. 6).

28

Fig. 7 shows the corresponding rejection rate and energy consumption for different percentage of permeate recycle. As the concentration of final permeate decreases, both the corresponding NDMA rejection and energy consumption are increased. At the highest permeate recycle (50%), the rejection is 93.1%, recovery is 24.7%, the final permeate concentration is 6.91×10^{-8} kg/m³, the energy consumption is 5.655 kWh/m³ (Figs. 6 and7). Interestingly, this rejection and permeate concentration are close to those of Configuration A4 but the recovery rate is much higher. This higher recovery is achieved not only due to permeate recycle by also at the expense of higher energy consumption. Also note, the NDMA rejection rate 93.1% is higher than that reported by Fujioka et al. [14] which was 92%. Although the recovery rate and energy consumption were not explicitly mentioned by Fujioka et al. [14], the 92% NDMA rejection was achieved at the expense of reduced membrane permeability between 20 – 35% for several types of membranes at the same selected feed concentration of 1000 ng/L.

From Figs. 6 and 7, it can be observed that 92.17% rejection can be achieved with permeate recycle of 30%, which gives a recovery rate of 34.82%, final permeate concentration of 7.827×10^{-8} kg/m³ and energy consumption of 3.466 kWh/m³. The rejection achieved is similar to that of solution 1 of configuration A (Table 5). However, the permeate recycle approach of configuration F increases the recovery rate by around 40% compared to configuration A at almost the same energy consumption.
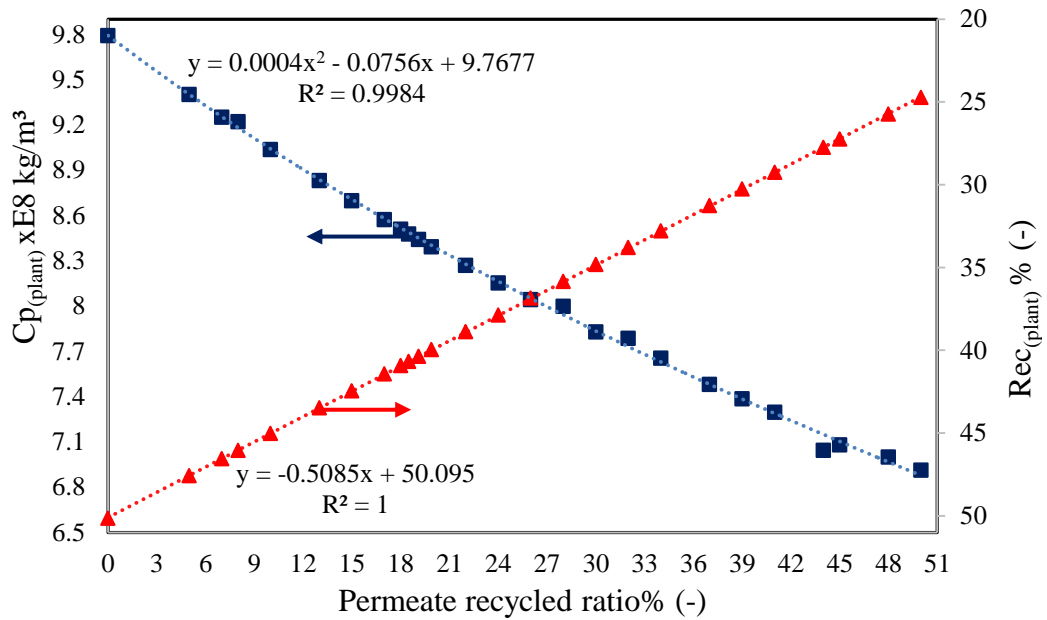
Fig. 6. The impact of permeate recycle on the plant NDMA concentration and total permeate recovery rate
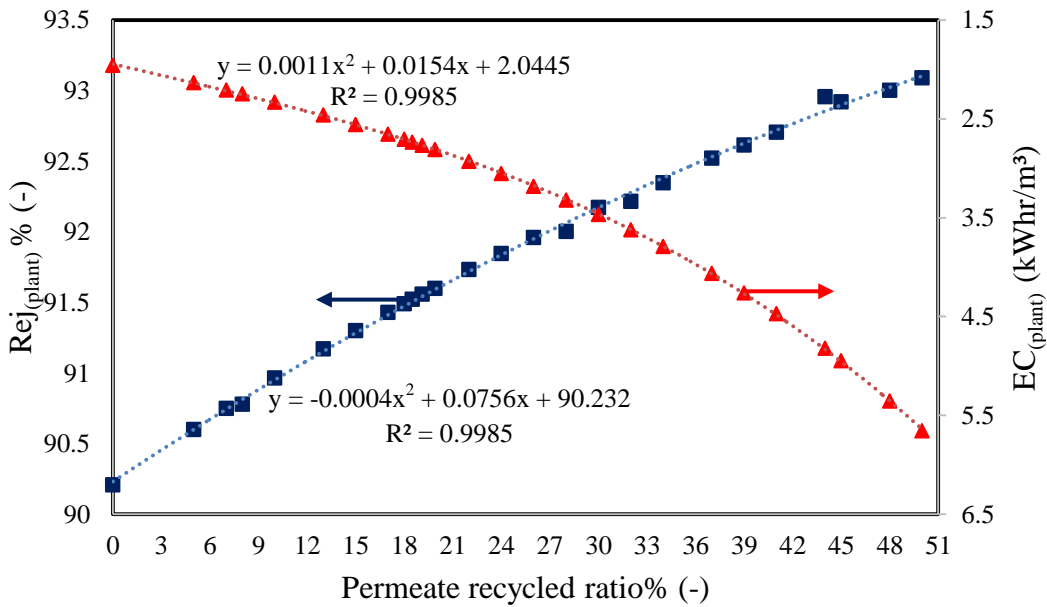

Fig. 7. The impact of permeate recycle on the plant NDMA rejection and total energy consumption

The simulation results presented in Figs. 6 and 7 are fitted with the following mathematical equations:

$$Cp_{(plant)} x10^8 = 0.0004\ (PR\%^2) - 0.0756\ (PR\%) + 9.7677 \tag{32}$$

$$Rec_{(plant)}\% = -0.5085\ (PR\%) + 50.095 \tag{33}$$

$$Rej_{(plant)}\% = -0.0004\ (PR\%^2) + 0.0756\ (PR\%) + 90.232 \tag{34}$$

$$EC_{(plant)} = 0.0011\ (PR\%^2) + 0.0154\ (PR\%) + 2.0445 \tag{35}$$

The proposed equations are only function of a single variable of permeate recycle ratio for the proposed configuration F. These equations can be used to estimate the final permeate concentration, recovery rate, rejection or energy consumption for a given permeate recycle rate albeit for the considered operating conditions of this research. However, the authors believe that it would be possible to employ it in the prediction of the performance indicators for the RO process at different operating data, which will be investigated in future research. Specifically, for a specified permeate concentration, Eq. (32) can be used to determine the required permeate recycle ratio and the corresponding recovery and energy consumption of the proposed design. For a given parameter, the above equations will provide an opportunity to estimate the remaining parameters with little effort. For example, for a recovery rate of 44.39 % (same as C2 of Table 5), the permeate recycle rate will be 11.22%, permeate concentration will be 8.9698x10^{-8} kg/m³, NDMA rejection will be 91.03% and energy consumption will be 2.355 kWh/m³. Note the NDMA rejection achieved and permeate concentration are better than those of C2 of Table 5 although the energy consumption is slightly higher.

Clearly configuration F shows an improvement not only over configuration C but other configurations too.

To summarise, it is fair to say that the implementation of the proposed configuration of permeate reprocessing and recycle mode in multistage RO process would deliver high advantages towards the efficient removal of NDMA from wastewater which is systematically approved to be within $40 - 70\%$. It must be stressed that the proposed configurations of RO system have not been used in practice yet to remove NDMA from wastewater and remain therefore theoretical at this stage. Also, the modelling equations developed in this work can be easily used to determine the required permeate recycle rate and to estimate the corresponding final permeate concentration and the energy consumption for a given NDMA rejection.

7. Conclusions

In this work, several configurations with multi-stage RO permeate reprocessing option are proposed and optimised in terms of NDMA removal from wastewater and energy consumption. For this purpose, a high fidelity mathematical model is developed and incorporated within a multi-objective optimisation framework using Species Conserving Genetic Algorithm (SCGA) to simultaneously maximise the rejection and minimise the total energy consumption subject to a number of process constraints. The mathematical model is validated against reliable experimental data and showed a good agreement. Amongst all the configurations considered, the best one is chosen based on its relative merit in terms of NDMA rejection (or final permeate concentration), recovery rate and energy consumption. The best configuration is then enhanced by adding the option of permeate recycling to the feed stream. Clearly, the new configuration with permeate reprocessing and recycling option offers an added benefit compared to other configurations with only the permeate reprocessing option. Finally, a series of simulation analyses are carried out for this configuration using different permeate recycle rate, and the

obtained NDMA rejection, final permeate concentration, recovery rate and energy consumption

are fitted with polynomial and linear equations which can be used as decision making tools.

Nomenclature

A : Effective area of the membrane (m²)

$A_{w(T)}$: Solvent transport coefficient at any temperature (m/atm s)

$A_{w(T_0)}$: Solvent transport coefficient at reference temperature (m/atm s)

A' : The spacer characteristics (dimensionless)

$B_{s(T)}$: Solute transport coefficient at any temperature (m/s)

$B_{s(T_0)}$: Solute transport coefficient at reference temperature (m/s)

C_b : The bulk feed solute concentrations at the feed channel (kg/m³)

C_f : The inlet feed solute concentrations at the feed channel (kg/m³)

$C_{f(plant)}$: The feed concentration of the plant (kg/m³)

C_m : The solute concentration on the membrane surface at the feed channel (kg/m³)

C_p : The permeate solute concentration at the permeate channel (kg/m³)

$C_{p(plant)}$: The product concentration of NDMA (kg/m³)

C_r : The retentate concentration of a membrane module (kg/m³)

C_{td} : The total drag coefficient (dimensionless)

D_b : The solute diffusion coefficient of feed at the feed channel (m²/s)

d_h : The hydraulic diameter (m)

EC : The total energy consumption of the whole plant (kWh/m³)

J_s : The solute molar flux through the membrane (kg/m² s)

J_w : The permeate flux (m/s)

k : The mass transfer coefficient at the feed channel (m/s)

K : The efficiency of mixing net (i.e. spacer) (dimensionless)

L : The length of the membrane (m)

m_f : Parameter in Eq. (10)

Mwt : Molecular weight (g/mol)

n : The spacer characteristics (dimensionless)

$P_{f(in)}$: The inlet feed pressure of a membrane module (atm)

$P_{f(in)(ERD)}$: The inlet pressure of ERD (atm)

$P_{f(plant)}$: The inlet feed pressure of the plant (atm)

$P_{f(out)}$: The outlet feed pressure of a membrane module (atm)

$P_{f(out)(ERD)}$: The outlet pressure of ERD (atm)

P_p : The permeate channel pressure of a membrane module (atm)

Q_b : The bulk feed flow rate at the feed channel of a membrane module (m³/s)

Q_f : The inlet feed flow rate at the feed channel of a membrane module (m³/s)

$Q_{f(plant)}$: The inlet feed flow rate of the plant (m³/s)

Q_p : The permeate flow rate at the permeate channel of a membrane module (m³/s)

$Q_{p(Plant)}$: The permeate flow rate of the plant (m³/s)

Q_r : The retentate flow rate at the feed channel of a membrane module (m³/s)

Re : The Reynold number at the feed channel (dimensionless)

Rec : Total permeate recovery of a membrane module (dimensionless)

$Rec_{(plant)}$: The total recovery rate of the plant (dimensionless)

Rej : The solute rejection coefficient of a membrane module (dimensionless)

$Rej_{(NDMA)}$: The plant total rejection of NDMA (dimensionless)

T : The feed temperature of a membrane module (°C)

$T_{(plant)}$: The inlet feed temperature of the plant (°C)

T_{ref} : The reference temperature (°C)

t_f : Height of feed channel (m)

U_b : The bulk feed velocity at the feed channel of a membrane module (m/s)

W : The membrane width (m)

Greek letters

μ_b : The Feed viscosity at the feed channel of a membrane module (kg/m s)

ρ_b : The feed density at the feed channel of a membrane module (kg/m³)

ΔL : The characteristic length of mixing net (m)

ΔP_{drop} : The pressure drop of the spiral wound element (atm)

$\Delta \pi_{Total}$: The osmotic pressure difference (atm)

π_m : The osmotic pressure at the membrane wall (atm)

π_p : The osmotic pressure at the permeate channel (atm)

ε_{pump} : Pump efficiency (dimensionless)

ε_{ERD} : Energy recovery device efficiency (dimensionless)

ϵ : The void fraction of the spacer (dimensionless)

References

[1] D. Bixio, C. Thoeye, J. De Koning, D. Joksimovic, D. Savic, T. Wintgens, T. Melin, Wastewater reuse in Europe. Desalination 187 (2006) 89–101.

[2] M. Gągol, A. Przyjazny, G. Boczkaj, Wastewater treatment by means of advanced oxidation processes based on cavitation – A review. Chemical Engineering Journal 338 (2018) 599–627.

[3] X. Chen, G. Huang, C. An, Y. Yao, S. Zhao, Emerging N-nitrosamines and N-nitramines from amine-based post combustion CO_2 capture – A review. Chemical Engineering Journal 335 (2018) 921–935.

[4] M. Krauss, P. Longrée, F. Dorusch, C. Ort, J. Hollender, Occurrence and removal of N-nitrosamines in wastewater treatment plants. Water Research 43 (2009) 4381–4391.

[5] A. Hebert, D. Forestier, D. Lenes, D. Benanou, S. Jacob, C. Arfi, L. Lambolez, Y. Levi, Innovative method for prioritizing emerging disinfection by-products (DBPs) in drinking water on the basis of their potential impact on public health. Water Research 44 (2010) 3147–3165.

[6] US EPA, United States Environmental Protection Agency IRIS database, (2009) https://www.epa.gov/iris.

[7] California Department of Public Health, Drinking Water Notification Levels and Response Levels: An Overview. State Water Resources Control Board—Division of Drinking Water (2015). http://www.waterboards.ca.gov/drinking_water/programs/

[8] Ontario's Ministry of the Environment, Technical Support Document for Ontario Drinking Water Standards, Objectives and Guidelines. 2003

[9] M. Krauss, P. Longrée, E. Van Houtte, J. Cauwenberghs, J. Hollender, Assessing the fate of nitrosamine precursors in wastewater treatment by physicochemical fractionation. Environ. Sci. Technol. 44 (2010) 7871–7877.

[10] T. Fujioka, *Assessment and optimisation of N-nitrosamine rejection by reverse osmosis for planned potable water recycling applications*. Ph.D. Theses, 2014. University of Wollongong.

[11] E. Steinle-Darling, M. Zedda, M.H. Plumlee, H.F. Ridgway, M. Reinhard, Evaluating the impacts of membrane type, coating, fouling, chemical properties and water chemistry on reverse osmosis rejection of seven nitrosoalklyamines, including NDMA. Water Research 41 (17) (2007) 3959–3967.

[12] M.H. Plumlee, M. Lo´pez-Mesas, A. Heidlberger, K.P. Ishida, M. Reinhard, N-nitrosodimethylamine (NDMA) removal by reverse osmosis and UV treatment and analysis via LC–MS/MS. Water Research 42 (2008) 347–355.

[13] T. Fujioka, S.J. Khan, J.A. Mcdonald, A. Roux, Y. Poussade, J. E. Drewes, L. D. Nghiem, Modelling the rejection of N-nitrosamines by a spiral-wound reverse osmosis system: Mathematical model development and validation. Journal of Membrane Science 454 (2014) 212–219.

[14] T. Fujioka, K.P. Ishida, T. Shintani, H. Kodamatani, High rejection reverse osmosis membrane for removal of N-nitrosamines and their precursors. Water Research 131 (2018) 45–51.

[15] Y. Magara, A. Tabata, M. Kohki, M. Kawasaki, M. Hirose, Development of boron reduction system for sea water desalination. Desalination 118 (1998) 25–33.

[16] J. Redondo, M. Busch, J. De Witte, Boron removal from seawater using FILMTECTM high rejection SWRO membranes. Desalination 156 (2003) 229–238.

[17] A. Farhat, F. Ahmad, N. Hilal, H.A. Arafat, Boron removal in new generation reverse osmosis (RO) membranes using two-pass RO without pH adjustment. Desalination 310 (2013) 50–59.

[18] F. Fang, B.-J. Ni, W.-M. Xie, G.-P. Sheng, S.-G. Liu, Z.-H. Tong, H.-Q. Yu, An integrated dynamic model for simulating a full-scale municipal wastewater treatment plant under fluctuating conditions. Chemical Engineering Journal 160 (2010) 522–529.

[19] C. Guria, P.K. Bhattacharya, S.K. Gupta, Multi-objective optimization of reverse osmosis desalination units using different adaptations of the non-dominated sorting genetic algorithm (NSGA). Computer and Chemical Engineering 29 (2005) 1977–1995.

[20] Z.V.P. Murthy, J.C. Vengal, Optimization of a reverse osmosis system using genetic algorithm. Sep. Sci. Technol. 41 (2006) 647–663.

[21] B. Djebedjian, H. Gad, I. Khaled, M.A. Rayan, Optimization of reverse osmosis desalination system using genetic algorithms technique, in: Twelfth International Water Technology Conference, IWTC12, Alexandria, Egypt, 2008.

[22] T.-M. Lee, H. Oh, Y.-K. Choung, S. Oh, M. Jeon, J.H. Kim, S.H. Nam, S. Lee, Prediction of membrane fouling in the pilot-scale microfiltration system using genetic programming. Desalination 247 (2009) 285–294.

[23] S.-M. Park, J. Han, S. Lee, J. Sohn, Y.-M. Kim, J.-S. Choi, S. Kim, Analysis of reverse osmosis system performance using a genetic programming technique, Desalination and Water Treatment 43 (2012) 281–290.

[24] A. Okhovat, S.M. Mousavi, Modelling of arsenic, chromium and cadmium removal by nanofiltration process using genetic programming. Appl. Soft Comput. 12 (2012) 793–799.

[25] R. Soleimani, N.A. Shoushtari, B. Mirza, A. Salahi, Experimental investigation, modeling and optimization of membrane separation using artificial neural network and multi-objective optimization using genetic algorithm. Chem. Eng. Res. Des. 91 (2013) 883–903.

[26] M.A. Al-Obaidi, J-P. Li, C. Kara-Zaïtri, I.M. Mujtaba, Optimisation of reverse osmosis based wastewater treatment system for the removal of chlorophenol using genetic algorithms. Chemical Engineering Journal 316 (2017) 91–100.

[27] J.H. Holland, Adaptation in Natural and Artificial Systems, University of Michigan Press, Ann Arbor, MI, 1975.

[28] K.A. De Jong, An Analysis of Behavior of a Class of Genetic Adaptive Systems. *Ph.D. thesis, University of Michigan, Ann Arbor, Michigan*, 1975.

[29] D.E. Goldberg, J. Richardson, Genetic algorithms with sharing for multimodal function optimization. *In Grefenstette, J. J., editor, Genetic Algorithms and their Applications: Proceedings of the Second International Conference on Genetic Algorithms*, pages 41–49, Lawrence Earlbaum, Hillsdale, New Jersey, 1987.

[30] J.P. Li, M. Balazs, G. Parks, P. Clarkson, A Species Conserving Genetic Algorithm for Multimodal Function Optimization. Evolutionary Computation 10 (3) (2002) 207–234.

[31] Q-F. Liu, S.-H. Kim, Evaluation of membrane fouling models based on bench-scale experiments: A comparison between constant flowrate blocking laws and artificial neural network (ANNs) model. Journal of Membrane Science 310 (2008) 393–401.

[32] M.A. Al-Obaidi, C. Kara-Zaïtri, I.M. Mujtaba, Development and Validation of N-nitrosamine Rejection Mathematical Model Using a Spiral-wound Reverse Osmosis Process. Chemical Engineering Transactions 52 (2016) 1129–1134.

[33] M.A. Al-Obaidi, C. Kara-Zaïtri, I.M. Mujtaba, Simulation of full-scale reverse osmosis filtration system for the removal of N-nitrosodimethylamine from wastewater. Asia-Pacific Journal of Chemical Engineering e2167 (2017) 1–13.

[34] H.K. Lonsdale, U. Merten, R.L. Riley, Transport properties of cellulose acetate osmotic membranes. J. Appl. Polym. Sci. 9 (1965) 1341–1362.

[35] Y. Winograd, A. Solan, M. Toren, Mass-transfer in narrow channels in presence of turbulence promoters, Desalination 13(2) (1973) 171–186.

[36] P.P. Mane, P.-K. Park, H. Hyung, J.C. Brown, J.-H. Kim, Modelling boron rejection in pilot- and full-scale reverse osmosis desalination processes. Journal of Membrane Science 338 (2009) 119–127.

[37] C. Koroneos, A. Dompros, G. Roumbas, Renewable energy driven desalination systems modelling. J. Cleaner Prod. 15 (2007) 449–464.

[38] A.R. Da Costa, A.G. Fane, D.E. Wiley, Spacer characterization and pressure drop modelling in spacer-filled channels for ultrafiltration. Journal of Membrane Science 87 (1994) 79–98.

[39] B. Qi, Y. Wang, S. Xu, Z. Wang, S. Wang, Operating energy consumption analysis of RO desalting system: Effect of membrane process and energy recovery device (ERD) performance variables. Industrial and Engineering Chemistry Research 51 (2012) 14135–14144.

[40] P. Sarkar, D. Goswami, S. Prabhakar, P.K. Tewari, Optimized design of a reverse osmosis system with a recycle. Desalination 230 (2008) 128–139.

[41] Process System Enterprise Ltd. 2001. *gPROMS Introductory User Guide*. London: Process System Enterprise Ltd.

[42] A. Abbas, Simulation and analysis of an industrial water desalination plant. Chemical Engineering and Processing 44 (2005) 999–1004.

[43] K. Keyvanloo, M. Sedighi, J. Towfighi, Genetic algorithm model development for prediction of main products in thermal cracking of naphtha: Comparison with kinetic modeling. Chemical Engineering Journal 209 (2012) 255–262.

[44] J.P. Li, Truss topology optimization using an improved species-conserving genetic algorithm. Engineering Optimization 47(1) (2015) 107–128.